Scientific Research Publishing

Food and Nutrition Sciences, 2021, 12, 915-936
https://www.scirp.org/journal/fns
ISSN Online: 2157-9458
ISSN Print: 2157-944X

Nanoencapsulation of Antioxidant-Rich Fraction of Roasted *Moringa oleifera* L. Leaf Extract: Physico-Chemical Properties and *in Vitro* Release Mechanisms

Pierre Nobossé[1,2], Edith N. Fombang[1*], Damanpreet Singh[2], Carl M. F. Mbofung[1]

[1]Department of Food Science and Nutrition, National School of Agro-Industrial Sciences, ENSAI, University of Ngaoundere, Ngaoundere, Adamawa Region, Cameroon
[2]Pharmacology and Toxicology Laboratory, CSIR-Institute of Himalayan Bioresource Technology, Palampur, Himachal Pradesh, India
Email: *edfombang@yahoo.fr

How to cite this paper: Nobossé, P., Fombang, E.N., Singh, D. and Mbofung, C.M.F. (2021) Nanoencapsulation of Antioxidant-Rich Fraction of Roasted *Moringa oleifera* L. Leaf Extract: Physico-Chemical Properties and *in Vitro* Release Mechanisms. *Food and Nutrition Sciences*, **12**, 915-936.
https://doi.org/10.4236/fns.2021.129068

Received: August 16, 2021
Accepted: September 15, 2021
Published: September 18, 2021

Abstract

Nanocapsules (NC) of antioxidant rich fraction of roasted Moringa leaves were prepared using emulsion coacervation technique with alginate (ALG) and/or chitosan (CTS) as biopolymers. NC were characterized based on particle size, polydispersity index (PDI), zeta potential, encapsulation efficiency (EE) and loading capacity (LC). Substituting CTS with ALG in NC caused a reduction in particle size and PDI, and enhanced EE. Mean particle size dropped from 1209 nm in 1:3 to 413 nm in 3:1 ALG/CTS-NC; PDI decreased from 0.9% to 0.2% and zeta potential from −5.4 to −28.1 mV. The highest EE (87.6%) and LC (13%) were obtained with ALG-CTS-NC (3:1). ALG-NC were spherical while both CTS and ALG-CTS-NC were ovoid. ALG and ALG-CTS-NC were oil/water emulsions while CTS-NC formed water/oil emulsions. 60% and 70% of bioactives in ALG-CTS-NC (3:1) were released in simulated gastric and intestinal fluids respectively after 400 min. Release of antioxidants from NC is concentration-dependent (First order model) and involves simultaneously diffusion (Higuchi model), swelling (korsmeyer-Peppas model) and erosion (Hixson-Crowell model) mechanisms.

Keywords

Nanoencapsulation, Roasted Moringa Leaf Extract, Liquid-Liquid Partitioning, Antioxidant Activity, Phenolic Compounds, Physico-Chemical Properties, Release Mechanisms

1. Introduction

Nutraceutical properties of *Moringa oleifera* Lam. leaves have been attributed to their strong antioxidant activity (AOA) provided by phenolic compounds, particularly flavonoids [1]. Previously, we showed that methanolic and ethanolic extracts of 45-day-old Moringa leaves exhibited the best antioxidant potential [2]; furthermore, that roasting treatment significantly improved AOA of *M. oleifera* L. leaves compared to other treatments such as blanching, drying, and fermentation [3]. In this regard, extraction parameters were optimized in order to maximize the antioxidant recovery from roasted *M. oleifera* L. leaves [4]. However, polyphenolic antioxidants from plant extracts are generally characterized by poor solubility and chemical instability which remain major barriers to their bioavailability and clinical efficacy [5]. Consequently, their delivery through the oral route is prone to rapid degradation in the gastrointestinal conditions, resulting in low intestinal uptake and poor bioavailability [6] [7]. To improve the stability of these antioxidants and enhance their efficiency in formulated nutraceutical products, it is necessary to incorporate them into a protective matrix. In this regard, nanoencapsulation, an advanced mode of drug delivery has proven its efficiency in preserving functionality and maximizing bioavailability of bioactives [7] [8]. Nanocapsules provide a vehicle for controlled or sustained release of bioactives and a larger contact surface area for adherence that may improve intestinal uptake and bioavailability [7] [9]. Among nanoencapsulation methods, nanoemulsions are attractive delivery systems for polyphenols and antioxidants because they improve their stability, solubility and bioavailability [10]. Of the multiple techniques developed to prepare nanoemulsions, emulsion-coacervation is appealing since it combines emulsification and ionic gelation to entrap bioactives into a strong and modulable network [11]. This method employs electrically charged biopolymers such as alginate and chitosan for encapsulation of bioactives. Nanoparticles prepared using nontoxic, biodegradable, and biocompatible biopolymers are suitable for food applications [8]. Alginate, chitosan and alginate-chitosan nanocarriers are useful for controlled release of bioactives and have demonstrated their suitability for the effective encapsulation and delivery of polyphenolic compounds [5] [12]. In this study, nanocapsules were formulated with an antioxidant-rich fraction of roasted *M. oleifera* L. leaf extract using alginate and/or chitosan as carriers.

2. Materials and Methods

2.1. Collection and Processing of Moringa Leaves

Fresh leaves of *Moringa oleifera* L. were harvested at 45 ± 2 days after trees were pruned in our experimental garden in Ngaoundéré, Adamawa Region, Cameroon [2]. Harvested leaves were immediately transported to the laboratory, cleaned and spread on stainless steel trays (1 g/20 cm^2) in a torrefier (BCM TORRE PICENARDI (CR), Model Panacea 2430, Italy) and were roasted at

145˚C ± 5˚C for 25 min [4]. The roasted leaves were ground using a blender (Moulinex, Model LM242027) and sieved to obtain the roasted leaf powder with particles size less than 500 µm. The powdered sample was packaged in polyethylene bags and stored at −20˚C for further analysis.

2.2. Extraction

Roasted Moringa leaf powder was extracted by maceration using a magnetic stirrer (IKA C-MAG HS 4) set at 3000 rpm. Three grams (3 g) of the roasted leaf powder was weighed into a 500 mL conical flask and placed in a thermostatic water bath. Extraction was carried out in 70% aqueous ethanol at 60˚C for 40 minutes with the solid-liquid ratio fixed at (1/40, w/v) [4]. The resultant extract was filtered using filter paper (Whatman No 1), concentrated under reduced pressure at 40˚C and freeze-dried.

2.3. Purification of Crude Extract of Roasted Leaves of *Moringa oleifera* L. Using Solvent Extraction (Liquid-Liquid Partition)

Crude extract was purified using solvents of increasing polarity according to the procedure described by Qin *et al.* [13] with modifications. The freeze-dried crude extract was suspended in distilled water (1/1, w/w); this suspension was exhaustively partitioned in hexane in a separating funnel until the additional volume of hexane remained colorless. The resulting hexane-soluble extract was labelled as hexane fraction (HF). The remaining water layer was further exhaustively and successively partitioned in ethylacetate and finally in butanol, yielding respectively the ethylacetate (EF) and butanol fractions (BF). The water layer remaining after butanol partition was labelled as water fraction (WF). After partition and phase separation, all fractions were evaporated to dryness under reduced pressure at 35˚C - 60˚C. The dried fractions resulting from this step were freeze-dried and stored in amber glass vials in a freezer until analyzed. To evaluate phenolic content and antioxidant activity, each fraction was quantitatively re-dissolved in methanol and analyzed for total phenolic content, total flavonoid content and antioxidant activity.

2.4. Determination of Total Phenolic and Flavonoid Content in Extract and Fractions

2.4.1. Sample Preparation

A stock solution of each extract (5 mg/mL) was prepared by dissolving the indicated mass of extract in methanol. Next, serial dilutions (0.1, 0.25, 0.5, 1, 2.5 and 5 mg/mL) were prepared from the stock solution and used in determination of phenolic content and antioxidant activity.

2.4.2. Total Phenolic Content

The total phenolic content of the extracts was determined as reported previously [14] using the Folin-Ciocalteu phenol reagent, with gallic acid as standard. The

total phenolic content was expressed as milligram gallic acid equivalence (GAE)/mg of extract.

2.4.3. Total Flavonoid Content

Flavonoids were determined according to the aluminum chloride method as described previously [14]. Catechin (0.01%) was used as standard. The total flavonoids content of extracts was expressed as milligram Catechin Equivalence (CE) mg extract.

2.5. Determination of Antioxidant Activity in Extract and Fractions

Antioxidant properties were measured using free radical scavenging activity (DPPH and ABTS) and reducing potential (FRAP and TAC assays).

2.5.1. DPPH (2,2-Diphenyl-2-Picryl Hydrazyl) Scavenging Activity

The DPPH scavenging activity was measured using Brand-Williams [15] method as described by [14]. Ascorbic acid (0.01 - 0.1 mg/mL) was used as standard. The DPPH scavenging activity (%) was plotted against extract concentration and the IC_{50} value (mg/mL) which denotes the concentration of extract required to scavenge 50% of free radicals was calculated.

2.5.2. $ABTS^{+}$ Radical Scavenging Activity

Experiments were performed according to Re *et al.* [16] as described by Nobossé *et al.* [2]. The ABTS radical scavenging activity was calculated as percent inhibition and plotted against sample concentrations. Hence, the IC_{50} values were calculated. Ascorbic acid was used as reference antioxidant.

2.5.3. Total Antioxidant Capacity (TAC)

The total antioxidant capacity of Moringa leaves was evaluated by the method of [17] as described by [2]. Ascorbic acid was used as standard antioxidant and the total antioxidant capacity was expressed as milligram ascorbic acid equivalence per milligram of extract (mg AAE/mg extract).

2.5.4. Ferric Reducing Antioxidant Power (FRAP) Assay

The antioxidant potential of *M. oleifera* L. leaf extracts was equally determined by their ability to reduce iron using the ferrous ion reducing capacity method as described by Yen and Chen [18]. Ascorbic acid was used as reference and the FRAP was expressed as milligram ascorbic acid equivalence per milligram of extract (mg AAE/mg extract).

2.6. HPLC Quantification of Phenolic Compounds in Crude Extract and Fractions

The phenolic compounds in the crude extract and fractions having high AOA were analyzed using HPLC-PDA [4]. The dried sample was mixed with methanol (1 mg/mL). The solution was dried with anhydrous sodium sulfate and filtered through a 0.22 μm nylon membrane filter (Axiva). The analysis was per-

formed on a HPLC system (Shimadzu, Japan) with a LC-20AT HPLC pump, DGU-20A5 degasser, SIL-20A auto sampler and SPDM20A PDA detector and CTO-10ASvp column oven. A Bridge RP18 (Waters) analytical column (5 µm, 250 × 4.6 mm) was used with 20 µL injection volume. The column oven temperature was set at 30˚C. The PDA acquisition wavelength was in the range of 250 - 400 nm; the analog output channel A at wavelength 280 nm and analog output channel B at 360 nm, both with bandwidth 2 nm. The gradient elution was carried out using a water-acetic acid mixture, 97:3 v/v, pH = 2.3 (solvent A) and 100% methanol (solvent B), with a flow rate of 1 mL/min. The binary gradient elution system started at 0% solvent B for 1 min, then 2% - 15% B for 6 min, 15% - 50% B for 13 min, 50% - 60% B for 10 min, 60% - 80% B for 12 min, 80% - 100% B for 13 min and 100% - 0% B for 5 min for a total run time of 60 minutes. The column was equilibrated with 100% phase A for 5 min prior to the next sample injection. Identification of sample polyphenols was done by comparing their retention time and UV absorption spectra with external standards analyzed under the same chromatographic conditions. The quantification of phenolic compounds in the extract was based on the calibration curves obtained with varying concentrations of the reference external standards.

2.7. Nanoencapsulation of Antioxidant-Rich Fraction of Roasted Moringa Leaf Extract

Antioxidant rich fraction obtained from liquid liquid partitioning was used for nanoencapaulation.

2.7.1. Preparation of Polymers (Carriers) and Emulsifier Solutions

Sodium alginate solution (0.1%, w/v) was prepared by dispersing the required amount of sodium alginate in 0.1% acetic acid solution. Chitosan solution (0.1%, w/v) was prepared by agitating chitosan in an acetic acid solution (0.1%, v/v) at 23˚C - 27˚C for 12 hours. Polyvinyl alcohol (0.2%, w/v) was used as aqueous emulsifier while soy lecithin (1%) was used as oil emulsifier. Stock solutions of calcium chloride (1%, w/v) and sodium tripolyphosphate (1%, w/v) were used as cross-linking agents. All solutions were prepared using double distilled water and filtered through 0.45 µm pore size nylon filter (Axiva) prior to use.

2.7.2. Procedure for Nanoencapsulation

Moringa-loaded nanocapsules were prepared by emulsion-coacervation which consist in preparing an oil-in-water emulsion, followed by crosslinking using calcium chloride or sodium tripolyphosphate (TPP). Three types of nanocapsules, namely alginate nanocapsules, chitosan nanocapsules and alginate/chitosan nanocapsules were prepared. The oil phase was made of soy lecithin (0.5%, w/v) and the antioxidant-rich fraction of the roasted Moringa leaf extract (5%, w/v) in corn oil [19].

Alginate nanocapsules were prepared according to the method described by [20] with modifications. The aqueous phase was made of a mixture of sodium

alginate and polyvinyl alcohol (1:1, v/v). The oil phase was gradually dropped into the aqueous phase under continuous mechanical stirring followed by high shear homogenization (Ultraturrax T-10 B, IKA, Germany) at 10,000 rpm for 5 minutes. Thereafter, $CaCl_2$ (0% - 0.025%) was added dropwise into the resulting emulsion under stirring and homogenized for an additional 5 minutes. Finally, the preparation was subjected to a probing sonication process in pulsed mode at 40% amplitude for 3 minutes with a sequence of 10 s of sonication and 5 s of rest using a sonicator (Sonics Vibra cell, S & M 220 probe, Newtown, Australia) to form nano-sized droplets.

Chitosan nanocapsules were prepared according to the method described by [11] with modifications. The aqueous phase was made of a mixture of chitosan and polyvinyl alcohol (1:1, v/v). The chitosan oil/water emulsion was made by dispersing the oil phase into the aqueous phase under continuous mechanical stirring followed by high shear homogenization (Ultraturrax T-10 B, IKA, Germany) at 10,000 rpm for 5 minutes. Furthermore, TPP (0% - 0.025%, w/v, final concentration) was added dropwise into the resulting emulsion while stirring and homogenized for an additional 5 minutes. Finally, the preparation was subjected to a probing sonication process as described above for alginate nanocapsules.

For the alginate-chitosan nanocapsules, the aqueous phase was made of an equal volume of polyvinyl alcohol solution and alginate/chitosan mixture in a ratio varying from 4:0 to 1:3, w/w). The primary emulsion made of oil phase in aqueous phase was prepared by high shear homogenization (Ultraturrax T-10 B, IKA) at 10,000 rpm for 5 minutes. Furthermore, $CaCl_2$ (0.0125%, final concentration) was added dropwise into the resulting emulsion under stirring and the preparation was then subjected to a probing sonication process under similar conditions as with alginate nanocapsules. Blank nanocapsules were prepared similarly but without the addition of the fraction.

2.8. Characterization of Nanocapsules

Nanocapsules were evaluated for their encapsulation efficiency, loading capacity, particle size and stability, particle morphology and bioactive release profile.

2.8.1. Encapsulation Efficiency and Loading Capacity

Nanocapsules (100 mg) were dispersed into 3 mL of methanol. The mixture was vortexed for 5 min and the resulting suspension was stirred for 1 h on a magnetic stirrer. The suspension was then centrifuged at 3000 rpm for 5 minutes and the supernatant collected. The procedure was repeated and both supernatants were pooled. Antioxidants in supernatant were quantified by spectrophotometry at 260 nm (UV-VIS spectrophotometer, Eppendorf, Germany). The amount of antioxidant-rich fraction entrapped into the nanocapsules (NC) was calculated according to a calibration curve of UV absorption at 260 nm versus concentration of AO-rich fraction. Encapsulation efficiency (EE%) was determined as the proportion of entrapped amount on initial amount of antioxidants (Equation

(1)) and percent loading capacity (LC%) was calculated as the amount of entrapped antioxidants to amount of nanocapsules (Equation (2)).

$$\mathrm{EE}(\%) = \frac{\text{Amount of entrapped antioxidants}}{\text{Initial amount of antioxidants}} \times 100 \quad (1)$$

$$\mathrm{LC}(\%) = \frac{\text{Amount of entrapped antioxidants}}{\text{Amount of NanoCapsules}} \times 100 \quad (2)$$

2.8.2. Particle Size and Polydispersity Index and Zeta Potential Measurements

The mean particle diameters (Z average) and polydispersity index of nanocapsules were measured using a dynamic light scattering instrument (Zetasizer Nano ZS, Malvern Instruments, Malvern, UK). The samples were diluted 10 times using double distilled water and then loaded in a measurement cell without introducing air bubbles. Samples were equilibrated for 1 min at 25˚C inside the instrument before dynamic light backscattering (detection angle: 173˚) data were collected. Each individual measurement was an average of 13 runs and measurements were performed in triplicate. The average particle size was calculated by the instrument using the Einstein-Stokes equation, assuming that the nanoemulsion droplets were spherical.

2.8.3. Determination of Microstructure of Nanoemulsion

The microstructure of the nanoemulsions was observed by transmission electron microscopy (TEM). A drop of nanoemulsion was diluted by a factor of 20 and deposited onto a carbon support film on a gold grid. Excess sample was removed using adsorbent paper. After drying the sample at 25˚C for 15 min, micrographs were taken by a transmission electron microscope (Philips Tecnai 12 Bio Twin, UK) operating at 80 kV. Images were registered on Kodak film SO163 and the negative scanned (Canon, Canoscan 9950F) at a resolution of 600 dpi.

2.9. Determination of *in Vitro* Release Profile and Modelling

2.9.1. *In Vitro* Release Profile

The *in Vitro* extract release study was carried out using treated dialysis bag diffusion technique. The dialysis membrane was soaked in double distilled water for 12 h prior to use. *In Vitro* release studies of alginate/chitosan nanoparticles of antioxidant-rich fraction of Moringa were performed in simulated gastric fluid (SGF) made of KCl-HCl buffer (0.1 M, pH 2) and simulated intestinal fluid (SIF) made of phosphate buffer (0.1 M, pH 8). Nanocapsules (100 mg) were dispersed in 4 mL of double distilled water. The dialysis tubing containing the dispersed nanocapsules was placed in a conical flask containing 25 mL of corresponding buffer. The flask was shaken at 200 rpm on a horizontal shaking incubator (New Brunswick scientific, Edison, NJ, USA) maintained at 37˚C for 8 hours. Every 30 minutes, 500 µL of dissolution medium was withdrawn and was replenished with same volume of fresh media to maintain sink conditions. The concentration of AO-rich fraction of Moringa leaf extract released from nano-

capsules was assayed at 260 nm (UV/Visible spectrophotometer, Eppendorf, Germany). The standard curve was plotted to represent the intensity of UV absorbance as a function of the concentration of the AO-rich fraction of Moringa.

2.9.2. Modeling

In drug delivery systems, mathematical modeling plays an important role in elucidating the main drug release mechanisms [21]. The first order model describes whether bioactive release rate is concentration dependent. On the other hand, the Higuchi model assumes that diffusion (Fick law) is the main mechanism underlying bioactive release. Meanwhile, under experimental conditions the release mechanism can deviate from the Fick equation, following an anomalous behavior (non-Fickian). This anomalous behavior can either be swelling or erosion-controlled release and would follow either Korsmeyer-Peppas or Hixson-Crowell model respectively [22]. It is worth noting that the Higuchi model assumes that swelling or dissolution of the matrix is negligible while the Korsmeyer-Peppas model involves simultaneously diffusion and swelling release mechanism. Meanwhile, during the modelling of bioactive release mechanism using Korsmeyer-Peppas model, only the first 60% of release data should be considered to avoid incorporation of erosion effect.

2.9.3. First Order Model

First order kinetics describes the dissolution profile of bioactive from dosage forms in a way that release rate is proportional to the amount of bioactive remaining in its interior. Hence, the amount of bioactive released per unit of time diminishes with release time (Equation (3)) [22].

$$Q_t = Q_0 \mathrm{e}^{-kt} \tag{3}$$

where Q_t is the amount of bioactive released at time t, Q_0 is the initial amount of bioactive in the solution and K is the first order release constant. The linearization of Equation (3) using decimal logarithm results in Equation (4):

$$\log Q_t = \log Q_0 - \frac{Kt}{2.303} \tag{4}$$

In this way a graph of the decimal logarithm of the released amount of bioactive versus time will be linear.

2.9.4. Higuchi Model

Higuchi model describes the release of a bioactive from an insoluble matrix as a function of the square root of time based on Fickian diffusion (Equation (5)).

$$Q_t = K_H * \sqrt{t} \tag{5}$$

where, Q_t is the amount of bioactive released at time t and K_H is the Higuchi dissolution constant.

2.9.5. Korsmeyer-Peppas Model

Korsmeyer-Peppas is a semi-empirical model, relating exponentially the bioac-

tive released from swelling-controlled systems to the elapsed time (t) (Equation (6)). It is used to analyze the release of bioactives from polymeric dosage forms when the release mechanism is not well known or when more than one type of release phenomena could be involved [22].

$$Q_t = Kt^n \tag{6}$$

where K is a constant incorporating structural and geometric characteristics of the dosage form, Q_t is the fraction of bioactive released at time t and n is the diffusional exponent, indicative of the drug release mechanism. For a Fickian diffusion, $n = 0.5$ while $0.5 < n < 1$ in case of a non-fickian diffusion [21]. Introducing logarithm on both sides, Equation (6) will be written as Equation (7):

$$\log Q_t = \log K + n \log t \tag{7}$$

Consequently, a graphic of the logarithm of the released fraction of bioactive versus time will result in a straight line.

2.9.6. Hixson-Crowell Model

Hixson-Crowell model is derived from the assumption that the particle regular area is proportional to the cubic root of its volume [22]. This model is given by Equation (8)

$$\sqrt[3]{W_0} - \sqrt[3]{W_t} = K_{HC} t \tag{8}$$

where W_0 is the initial amount of bioactive in the dosage form, W_t is the remaining amount of bioactive in dosage form at time t and K_{HC} is the Hixson constant incorporating the surface-volume relation. A graphic of the cubic root of the unreleased fraction of bioactive versus time (Equation (9)) will be linear if the equilibrium conditions are not reached and if the geometrical shape of the pharmaceutical dosage form diminishes proportionally over time [22]. In this graph, K_{HC} is given by the slope of the straight line which intersects the ordinate axis at 1.

$$\sqrt[3]{\frac{W_t}{W_0}} = 1 - K_{HC} t \tag{9}$$

Then, introducing logarithm results in Equation (10) which is a linear form of Hixson-Crowell equation.

$$\log\left(\sqrt[3]{\frac{W_t}{W_0}}\right) = -\log K_N + \log t \tag{10}$$

where K_N is a modified Hixson constant which could be easily obtained as the intercept of the linear graphic of the logarithm of cubic root of the unreleased fraction of bioactive versus time.

2.10. Statistical Analysis

All measurements were performed in triplicate in each experiment. Results are presented as means ± SD. Statistical analysis was performed by one-way

ANOVA using Statgraphics centurion XVI and the Duncan multiple comparison test at 5% confidence level was used to check significant differences. SigmaPlot 11 (SYSTAT Software San Jose, CA) was used for plotting graphs.

3. Results and Discussion

3.1. Total Phenolic, Flavonoid Content and Antioxidant Activity of Crude Extract and Fractions of Roasted Moringa Leaf Extract

Four fractions namely hexane fraction (HF), ethylacetate fraction (EF), butanol fraction (BF) and water faction (WF) were obtained by the partial purification procedure. Total phenolic, total flavonoids content and antioxidant activity were determined in all fractions as well as the crude extract. **Figure 1(a)** depicts total phenolic and flavonoid content in the fractions obtained from liquid-liquid partitioning of roasted Moringa crude leaf extract. Radical scavenging activity and reducing power in the fractions are presented in **Figure 1(b)** and **Figure 1(c)** respectively.

Both EF and BF had higher phenolic and flavonoid concentrations than crude extract and all other fractions. Comparatively with crude extract, total flavonoid content in EF (0.38 mg CE/mg extract) and BF (0.28 mg CE/mg extract) was respectively 4 and 3 times higher, indicating that flavonoids are concentrated in the ethylacetate and butanol fraction during liquid-liquid partitioning. Likewise, total phenolic compounds initially present in crude extract (0.17 mg GAE/mg extract) were concentrated in EF (0.5 mg GAE/mg of fraction) and BF (0.41 mg GAE/mg of fraction). **Table 1** shows fraction yields as well as the distribution of total phenolics and flavonoids in different fractions. Both ethylacetate and butanol fractions contained 52.8% of total flavonoids and 41.4% of total phenolic present in crude extract. Similarly, higher AOA represented by low IC_{50} values for DPPH and ABTS were obtained with EF and BF. Compared to crude extract, IC_{50} for DPPH scavenging activity increased 3.1 times (0.41 mg/mL) and 2.1 times (0.59 mg/mL) in EF and BF respectively. Concurrently, ABTS scavenging activity was enhanced 2.6 and 2.1 times respectively in EF (0.42 mg/mL) and BF (0.51 mg/mL) compared to crude extract (1.1 mg/mL). Reducing potential and total antioxidant capacity were equally higher in EF (0.76 mg AAE/mg extract and 0.43 mg AAE/mg extract respectively) and BF (0.47 mg AAE/mg extract and 0.34 mg AAE/mg extract respectively). FRAP increased 3.2 and 2 folds while TAC increased 1.7 and 1.3 folds respectively in EF and BF compared to crude extract and the other fractions. The water fraction contained up to 35.9% and 29.6% of phenolic compounds and flavonoid respectively but had lowest AOA. The higher AOA in EF and BF is consistent with their higher concentration of TPC and TFC. Previous studies had shown positive correlation between TPC, TFC and AOA [2] [23] [24]. According to Qin *et al.* [13], polyphenols dissolved in ethylacetate and butanol fractions would be more polar and associated with more substituted hydroxyl groups and higher AOA compared to those that would preferably be partitioned in other fractions.

Table 1. Distribution of TPC and TFC in fractions.

	Fraction yield (%)	Total phenolic compounds		Total flavonoid compounds	
		Amount (g)	Proportion (%)	Amount (g)	Proportion (%)
Crude extract		17.66	100	9.7	100
Hexane fraction	25.45	3.07	17.42	1.27	13.11
Ethylacetate fraction	3.07	1.535	8.70	1.16	12.03
Butanol fraction	14.15	5.801	32.85	3.96	40.49
Water fraction	55.64	6.33	35.89	2.87	29.60

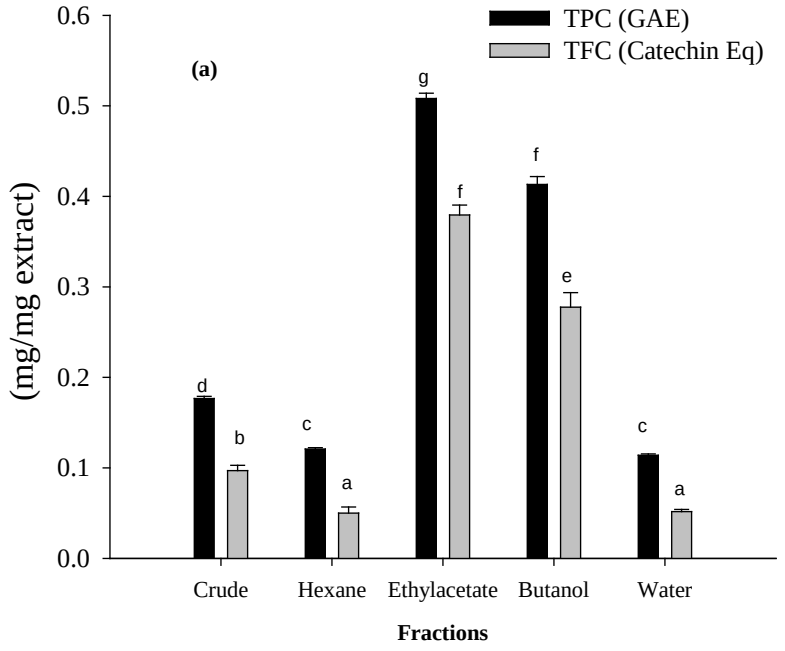

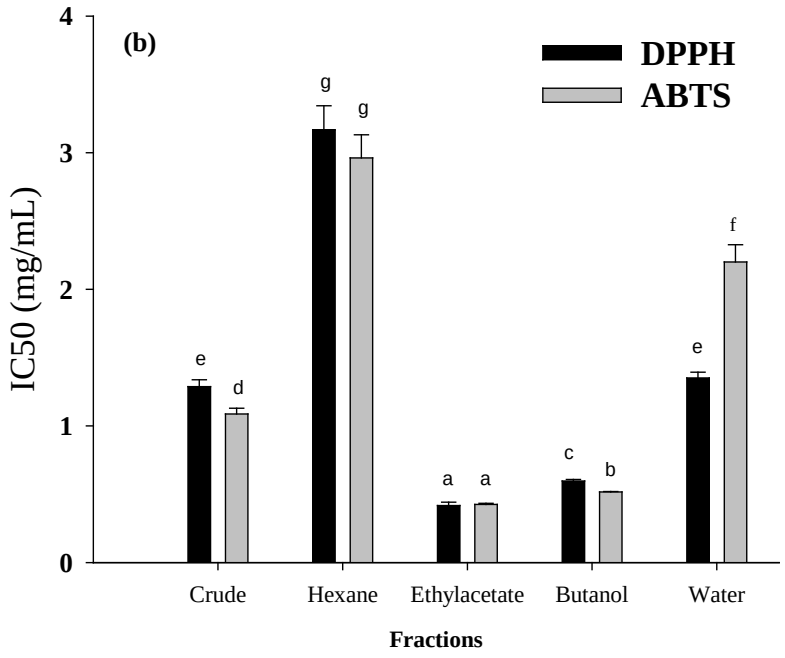

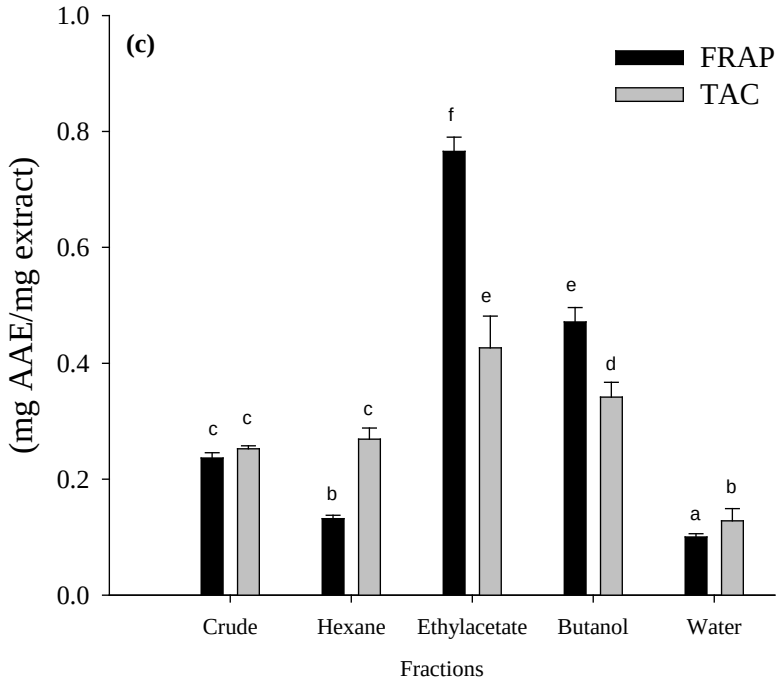

Figure 1. Total Phenolic content and Antioxidant activity in crude extract and fractions of the roasted *Moringa oleifera* L. leaf extract. TPC: Total phenolic content; TFC: Total flavonoid content; GAE: Gallic Acid Equivalent. (a) Total phenolic and flavonoid content; (b) DPPH and ABTS scavenging activity; (c) FRAP (Ferric Reducing Antioxidant Power) and TAC (Total Antioxidant Capacity) Different letters on the bars represent significant differences ($p < 0.05$).

Therefore, liquid-liquid partitioning can be used to partially purify crude polyphenols extracts; and in the case of Moringa concentrates polyphenols and AO potential in ethylacetate and butanol fractions. These results are in accordance with findings by [25] who reported higher concentration of phenolic compounds as well as antioxidant activity in ethylacetate fraction of Moringa leaf extract compared to crude extract. Similar results have also been obtained in *Viola tianshanica* where liquid-liquid partitioning led to concentration of most flavonoids and flavonoid glucosides in both ethylacetate and butanol fractions [13].

Given that most of the polyphenols and flavonoids were concentrated in the EF and BF, and that they equally had highest AOA, these two fractions were pooled together and considered as the antioxidant rich fraction that was used for the formulation of nanocapsules.

3.2. Identification and Quantification of Phenolic Compounds in Crude Extract and Antioxidant Rich Fractions of Roasted *Moringa oleifera* L. Leaves

HPLC profile of the crude extract and AO-rich fractions (EF and BF) of roasted *M. oleifera* L. leaves showed several peaks among which five phenolic compounds (caffeic acid, rutin, isoquercetin, quercetin, and vanillin) were successfully identified and quantified comparatively to external standards (**Table 2**).

Table 2. Identified phenolics in extract and fractions of roasted *M. oleifera* L. leaves.

RT* (min.)	UV abs.sple (nm)	UV abs.std (nm)	Identity	Concentration (mg/g extract)		
				CE**	EF	BF
3.1 ± 0.1	221, 235	219, 235	Vanillin	4.7 ± 0.9	1.7 ± 0.5	16.3 ± 0.3
20.0 ± 0.2	219, 247, 321	220, 245, 324	Caffeic acid	9.0 ± 2.0	-	5.6 ± 0.01
27.1 ± 0.1	227, 256, 355	221, 255, 356	Isoquercetin	10.4 ± 0.9	-	13.0 ± 0.1
27.7 ± 0.2	221, 255, 356	231, 256, 356	Rutin	45.0 ± 5.0	89.2 ± 1.4	14.9 ± 0.2
38.1 ± 0.4	214, 256, 369	219, 255, 372	Quercetin	15.2 ± 1.5	15.9 ± 0.5	16.7 ± 0.4

*mean value of 5 runs, RT: retention time; CE: crude extract; EF: ethylacetate fraction; BF: butanol fraction; **Fombang *et al.*, 2020.

Rutin (RT 27.7 min.) had the highest concentration (45 mg/g extract) in crude extract of roasted Moringa leaf, followed by quercetin (15.2 mg/g, RT 38.1 min), isoquercetin (10.4 mg/g, RT 27.1 min.), caffeic acid (9.0 mg/g, RT 20.0 min.) and vanillin (4.7 mg/g, RT 3.1 min.).

Comparatively to the crude extract, higher concentration of rutin (89.2 mg/g) and quercetin (15.9 mg/g) were identified in ethylacetate fraction. In addition to rutin (14.9 mg/g) and quercetin (16.7 mg/g) butanol fraction also contained considerable amounts of vanillin (16.2 mg/g) and isoquercetin (13 mg/g). In contrast to these findings, Verma *et al.*, [25] reported low concentration of quercetin (0.81 mg/g) and rutin (0.19 mg/g) in addition to other phenolic compounds such as gallic acid, chlorogenic acid, ellagic acid and ferulic acid in ethylacetate fraction of methanol leaf extract of *Moringa oleifera*.

High concentrations of rutin and quercetin, which are flavonoids having 3',4'-O-dihydroxy group in their structure in EF and BF (**Table 2**) could be responsible for the higher AOA (**Figure 1(b)** and **Figure 1(c)**) observed in these fractions. In fact, the number and positioning of the B-ring hydroxyl groups in flavonoids are important to their ROS (Reactive Oxygen Species) inhibitory effects [26]. Consequently, the presence of 3',4'-O-dihydroxy group is a good indicator of the ROS inhibitory activity and high antioxidant activity of flavonoids because of the intra-molecular hydrogen bonding between the 3',4'-O-dihydroxyls. Moreover, comparative analysis showed that quercetin and rutin have lower 4'-bond dissociation enthalpies than other flavonoids, indicative of their higher hydrogen atom donating ability [26].

3.3. Characterization of Nanocapsules

3.3.1. Mean Particle Size, Polydispersity Index and Mean Zeta Potential

The prepared nanocapsules were characterized based on their particle size, polydispersity index (PDI) and mean zeta potential (**Table 3**).

PDI is a quality parameter that indicates the uniformity of droplet size in nanoemulsions. Nanoparticles having PDI ≤ 0.1 are considered to be highly monodisperse while values comprised between 0.1 - 0.4 and >0.4 indicate respectively moderately and highly polydisperse particles [27]. Following addition of calcium

Table 3. Particle size, polydispersity index and zeta-potential of Moringa-based nanocapsules.

Alginate nanocapsules (ALG)	$CaCl_2$ ($\times 10^{-3}$%)	0	6.25	12.5	25
	Mean size (nm)	387 ± 10	274 ± 5	311 ± 5	273 ± 11
	PDI	0.46 ± 0.03	0.26 ± 0.03	0.27 ± 0.04	0.21 ± 0.02
	z-potential (mV)	−43.3 ± 0.1	−30.6 ± 0.6	−23.5 ± 0.7	−19.1 ± 0.5
Chitosan nanocapsules (CTS)	TPP ($\times 10^{-3}$%)	0	6.25	12.5	25
	Mean size (nm)	303 ± 15	487 ± 29	523 ± 52	2249 ± 176
	PDI	0.20 ± 0.01	0.48 ± 0.3	0.3 ± 0.05	0.6 ± 0.3
	z-potential (mV)	+50 ± 1	+33 ± 1	+24 ± 0.4	+13 ± 0.4
Alginate-chitosan nanocapsules (ALG-CTS)	ALG-CTS ratio	1:3	1:1	3:1	4:0
	Mean size (nm)	1209 ±160	488 ± 15	413 ± 4	394 ± 7
	PDI	0.90 ± 0.20	0.45 ± 0.03	0.20 ± 0.03	0.4 ± 0.1
	z-potential (mV)	−5.4 ± 0.1	−20.0 ± 0.8	−28.1 ± 0.7	−41.6 ± 0.1

PDI: polydispersity index, TPP: Sodium tripolyphosphate; ALG: Alginate; CTS: chitosan.

chloride in alginate nanocapsules, the PDI dropped in a concentration-dependent manner from 0.46 in nanocapsules without calcium chloride to 0.21 with 0.025% $CaCl_2$ solution; indicating that the addition of calcium chloride in alginate nanocapsules improves uniformity of particles in the emulsion.

On the contrary, addition of TPP in chitosan nanocapsules resulted in an increase in both particle size and PDI. High concentration of TPP (0.025%) caused formation of large and non-uniform particles with size and PDI as high as 2249 nm and 0.6 respectively (**Table 3**). The substitution of chitosan with alginate in alginate-chitosan nanocapsules resulted in a reduction of both particle size and PDI. For instance, the mean particle size dropped gradually from 1209 nm in alginate-chitosan nanocapsules (1:3, w/w) to 394 nm in those made exclusively of alginate (**Table 3**). Generally, in most of the formulations, the PDI was between 0.2 - 0.4, indicating that the nanocapsules were moderately disperse and had a narrow particle size distribution [8] [27].

Smaller particle sizes are desirable as it has been demonstrated that these are taken up and transported more efficiently across the intestinal cells than larger particles [7]. Moreover, it has been found that nano-sized particles are ideal for oral drug delivery since they are preferentially taken up by both enterocytes and epithelial cells, demonstrating higher intestinal transport compared to larger sized particles [9] [28].

Zeta potential is defined as the electric charge on particle surface which creates an electrical barrier and acts as a "repulsive factor" responsible for the stabilization of nanoparticles [29]. The high magnitude of zeta-potential (>10 mV in absolute) is a sign of high-energy barrier between particles and predicts good colloidal stability of prepared nanoemulsions [30]. The particle charge was inherently negative in both alginate and alginate-chitosan nanocapsules due to

the presence of free carboxyl residues in alginate. Alginate nanocapsules, made without addition of chitosan and/or calcium chloride were highly negatively charged with zeta potential values of −43.3 and −41.6 mV respectively. Conjugation of alginate with chitosan greatly increased the particle charge from −41.6 to −5.4 mV as well as did crosslinking with calcium chloride (from −43.3 to −19.1 mV). The loss of negative charge in ALG nanocapsules with conjugation or crosslinking suggests successful conjugation of chitosan and calcium to alginate molecules. It is indeed known that the charge of droplets in nanoemulsions can be altered by adsorption of other charged substances onto their surfaces [31]. Similarly, particle charge in chitosan nanocapsules decreased with cross-linking to sodium tripolyphosphate (TPP) from 50 mV in TPP-free nanocapsules to 13 mV in those containing 0.025% of TPP (**Table 3**); indicating an effective association between positively charged chitosan molecules and negatively charged TPP molecules.

3.3.2. Encapsulation Efficiency and Loading Capacity

When evaluating the suitability of biopolymer particles as encapsulation systems for a specific bioactive, the loading capacity (LC) and encapsulation efficiency (EE) are typically the most important factors of interest. The EE (%) of chitosan nanocapsules was lower (61%) compared to that of alginate nanocapsules (78%) (**Table 4**). Addition of a crosslinking agent in both cases improved the EE by 7% - 9% in alginate nanocapsules and 5% - 14% in chitosan nanocapsules. Combination of alginate and chitosan markedly enhanced EE (84% - 88%) compared to CTS nanocapsules (61% - 70%) but was similar to EE of calcium cross-linked ALG nanocapsules (83% - 85%). Similar observations were made with LC. Highest EE (87.6%) and LC (13%) were obtained for alginate-chitosan ratio of 3:1 (w/w) (**Table 4**). In addition to its low PDI (0.2) and high zeta-potential (−28.1 mV) (**Table 3**), this formulation stands out as the most relevant for nutraceutical application.

Our results show that both encapsulation efficiency and loading capacity varied with type of coating polymer as well as concentration of cross-linking agent, in accordance with previous observation that encapsulation efficiency may be influenced by both the polymers and the surfactants used [30]. The loading capacity on its part is highly dependent on the affinity between the biopolymer and bioactive compounds [32], as well as the physicochemical properties such as lipophile/hydrophile ratio of the bioactive [33]. Loading capacity as high as 52% was reported for encapsulation of coumarin 6 in poly (lactic-co-glycolic) nanoparticles by emulsification solvent evaporation method [33]. Loading capacity range of 37% - 100% was reported in alginate/chitosan nanoparticles depending on ALG/CTS ratio and calcium chloride proportion [34]. On the other hand, Tan *et al.* [35] reported maximum loading capacity of 1.6% for incorporation of β-carotene in liposomes. From a practical point of view, it is important to have the highest loading capacity of a nutraceutical within a delivery system [36].

Table 4. Encapsulation efficiency and loading capacity of nanocapsules.

Alginate nanocapsules			Chitosan nanocapsules			Alginate-chitosan nanocapsules		
$CaCl_2$ ($\times 10^{-3}$%)	EE (%)	LC (%)	TPP ($\times 10^{-3}$%)	EE (%)	LC (%)	ALG-CTS ratio	EE (%)	LC (%)
0	78.6 ± 1.9	12.4 ± 0.1	0	61.5 ± 1.0	9.3 ± 0.1	1:3	84.4 ± 1.1	12.8 ± 0.9
6.25	84.0 ± 1.5	12.7 ± 0.1	6.25	64.4 ± 1.6	9.3 ± 0.3	1:1	85.3 ± 0.6	12.2 ± 0.4
12.5	83.6 ± 2.0	12.4 ± 0.3	12.5	69.9 ± 1.6	10.2 ± 0.6	3:1	87.6 ± 0.8	13.1 ± 0.4
25	85.5 ± 0.6	11.9 ± 0.1	25	64.7 ± 1.2	10.1 ± 0.3	4:0	83.6 ± 2.0	12.9 ± 0.3

ALG: Alginate; CTS: chitosan; EE: Encapsulation Efficiency; LC: Loading Capacity; TPP: Sodium tripolyphosphate.

3.3.3. Microscopic Characteristics of Nanocapsules

To study the morphology, the shape and size distribution of nanoparticles, transmission electron microscopy (TEM) was used [37]. TEM micrographs of alginate, chitosan and alginate-chitosan nanocapsules (**Figure 2**) showed that the morphology of nanocapsules depends on the nature of polymer used for encapsulation. Alginate nanocapsules had a spherical shape while both chitosan and alginate-chitosan nanocapsules were ovoid. Both alginate and alginate-chitosan nanocapsules showed black oily inner droplet characteristic of oil-in-water emulsion while chitosan nanocapsules formed water-in-oil emulsion characterized by aqueous whitish inner phase. Moreover, TEM images showed particles size ranging from 100 to 1000 nm, in accordance with the size obtained from dynamic light scattering.

3.3.4. *In Vitro* Release Profile

Alginate-chitosan (3:1, w/w) nanocapsules which showed high encapsulation efficiency, loading capacity, zeta potential and low PDI were used to study the release profile of bioactives from nanocapsules in simulated gastric fluid (SGF) and simulated intestinal fluid (SIF). Bioactives release from nanocapsules occurred in a controlled manner and was characterized by three phases (**Figure 3**). An initial low-release rate phase lasting about 30 minutes with about 5% of bioactives released. This was followed by an exponential-release phase lasting up to 400 minutes with 60% or 70% of bioactives released in SGF and SIF respectively. Beyond this point, was a stable phase where no additional release of bioactives occurred.

In the second phase, the release profile was significantly ($p < 0.05$) influenced by pH with more bioactives being released in alkaline (SIF) than in acidic (SGF) medium. This observation is in line with the fact that sodium alginate used as coating material shrinks in acidic medium but degrades in alkaline medium [38], thus lowering the diffusion of encapsulated active substance from inner to outer surface in SGF and favoring greater release in the intestine (SIF). The absence of a burst effect at the initial phase is evidence of the absence of uncoated bioactive on the surface of nanocapsules and also of earlier degradation of the coating polymer; given that the burst effect is attributed either to desorption of the drug

located on the surface of nanocapsules [39], or to the degradation of the thin polymeric membrane [40]. Similar observation of the absence of initial burst phase was reported during the release of rutin from ferritin-rutin-EGCG nanoparticles [41]. The absence of a burst effect disagrees with previous observations that the release profile from nanocapsules obtained by emulsion-coacervation is biphasic and characterized by a fast initial (burst) phase followed by a slower second phase corresponding to the diffusion of bioactive molecules from the inner compartment to the outer phase [40] [42]. This difference can be explained by the nature of encapsulate and coating polymers, the method of nanocapsules preparation and interactions between encapsulate and coating polymer [30]. The incomplete release observed in this study (**Figure 3**) may be attributed either to the retention capacity of the targeted antioxidants on polymer matrix [40] or to the saturation of diffusion media [43].

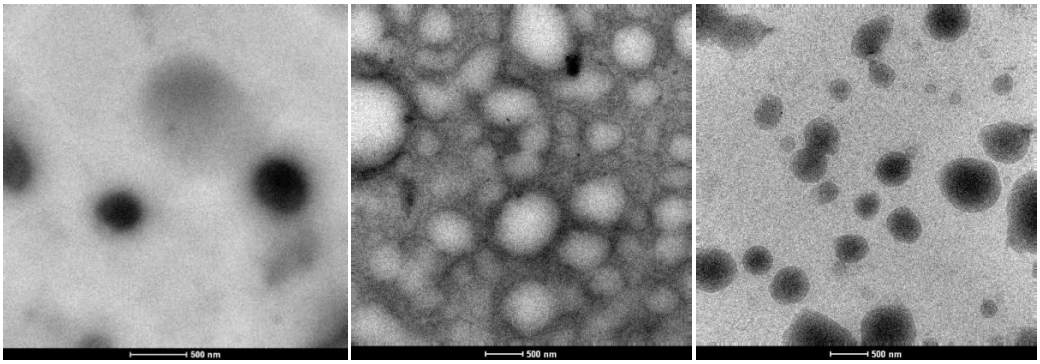

(a) (b) (c)

Figure 2. Transmission electron micrographs of nanocapsules. (a) Alginate nanocapsules, (b) chitosan nanocapsules and (c) alginate-chitosan (3:1, w/w) nanocapsules.

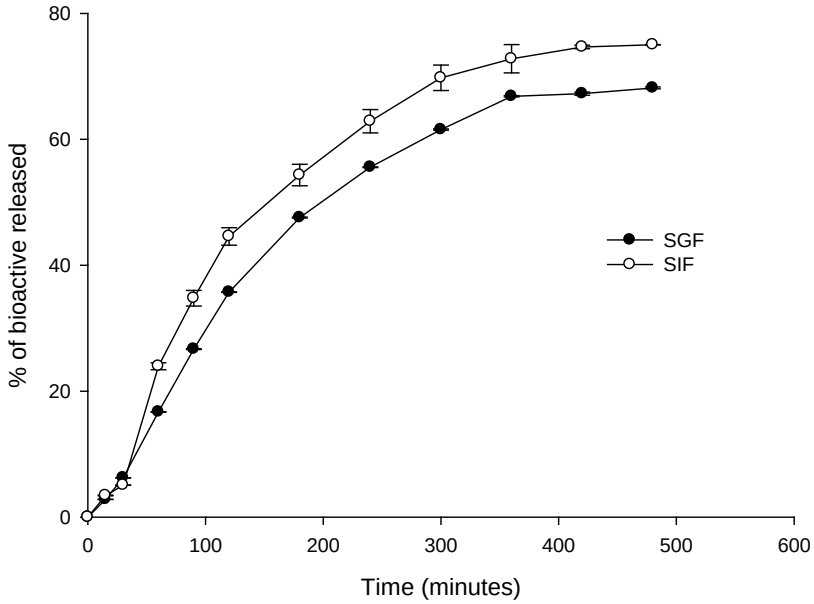

Figure 3. Antioxidants release profile from nanocapsules in simulated gastric fluid (SGF) and simulated intestinal fluid (SIF).

3.3.5. Modelling of Bioactive Release Profile

The mathematical modeling of bioactive release profile from the nanocapsules is described by Figure 4 using first order (a), Higuchi (b), Korsmeyer-Peppas (c) and Hixson-Crowell (d) models. The validity of these models was evaluated according to goodness of fit based on correlation coefficients. High correlation coefficients ($R^2 > 0.9$) indicate strong fit of antioxidant release profile to the tested models. The release profile was most adequately fitted to Korsmeyer-Peppas model ($R^2 = 0.94 - 0.97$). According to values of correlation coefficients, all tested models were valid and could be adequately used to represent the release of antioxidants from Moringa-loaded nanocapsules. Based on these models, it can be affirmed that the release of antioxidants from Moringa-loaded nanocapsules is concentration-dependent (First order model) and involves both diffusion (Higuchi model), swelling (korsmeyer-Peppas model) and erosion (Hixson-Crowell model) mechanisms.

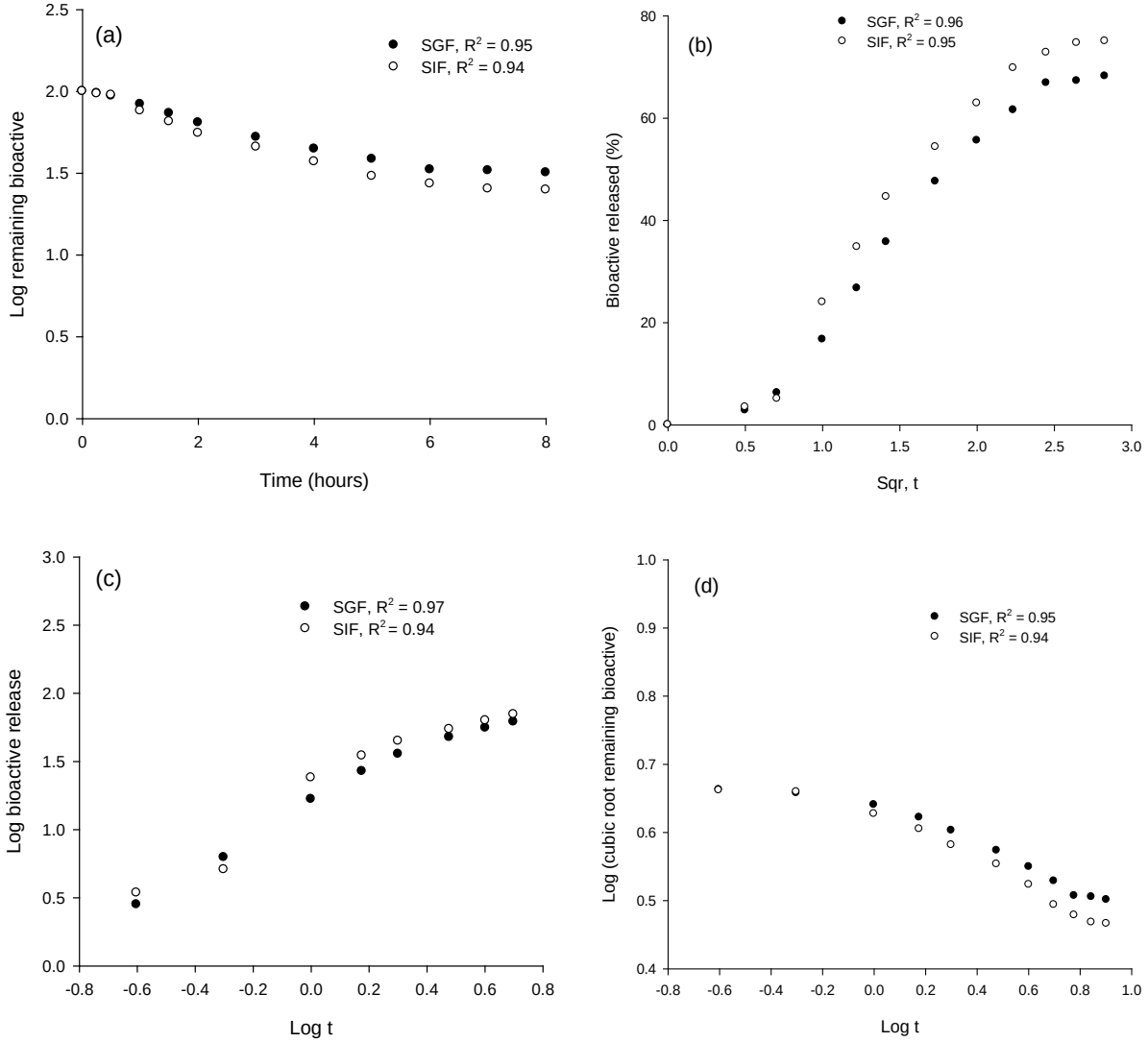

Figure 4. Modelling of antioxidants release mechanism from Moringa loaded nanocapsules. (a) First order model; (b) Higuchi model; (c) Korsmeter-Peppas model; (d) Hixson-Crowell model.

4. Conclusion

Partial purification and concentration of bioactives (polyphenols, flavonoids and AOA) in roasted *M. oleifera* Lam leaf extract can be obtained using liquid-liquid partitioning. Both ethylacetate and butanol fractions of roasted *Moringa oleifera* L. leaf extract exhibited the most relevant antioxidant activity supported by the highest phenolic and flavonoid content. Nanoencapsulation of this antioxidant-rich fraction using emulsion-coacervation technique resulted in stable nanoparticles. Encapsulation efficiency and loading capacity depend on the nature of coating polymer and concentration of cross-linking agent. Combining sodium alginate with chitosan yields nanocapsules with higher encapsulation efficiency. Nanocapsules made of alginate are spherical while those made of chitosan and alginate-chitosan mixture are ovoid. The release of antioxidants from Moringa-loaded alginate-chitosan nanocapsules is concentration-dependent and involves simultaneously diffusion, swelling and erosion mechanisms.

Acknowledgements

The authors acknowledge financial support to Mr. Nobossé by The World Academy of Science (TWAS) and the Council for Scientific and Industrial Research (CSIR), India through the TWAS-CSIR postgraduate fellowship program (FR number: 3240280447). The authors are also grateful to the Director, CSIR-Institute of Himalayan Bioresource Technology, Palampur, H.P. India for providing the research facilities.

Conflicts of Interest

The authors declare no conflicts of interest regarding the publication of this paper.

References

[1] Gopalakrishnan, L., Doriya, K. and Kumar, D.S. (2016) *Moringa oleifera*: A Review on Nutritive Importance and Its Medicinal Application. *Food Science and Human Wellness*, **5**, 49-56. https://doi.org/10.1016/j.fshw.2016.04.001

[2] Nobossé, P., Fombang, E.N. and Mbofung, C.M.F. (2018) Effects of Age and Extraction Solvent on Phytochemical Content and Antioxidant Activity of Fresh *Moringa oleifera* L. Leaves. *Food Science & Nutrition*, **6**, 2188-2198. https://doi.org/10.1002/fsn3.783

[3] Fombang, E.N., Nobossé, P., Mbofung, C.M.F. and Damanpreet, S. (2021) Impact of Post Harvest Treatment on Antioxidant Activity and Phenolic Profile of *Moringa oleifera* Lam Leaves. *Food Production*, *Processing and Nutrition*, **3**, Article No. 22. https://doi.org/10.1186/s43014-021-00067-9

[4] Fombang, E. N., Nobossé, P., Mbofung, C. M. F. and Damanpreet, S. (2020) Optimising Extraction of Antioxidants from Roasted *Moringa oleifera* Lam. Leaves Using Response Surface Methodology. *Journal of Food Processing & Preservation*, **44**, Article No. e14482. https://doi.org/10.1111/jfpp.14482

[5] Ratul, K.D., Naresh, K. and Utpal, B. (2010) Encapsulation of Curcumin in Alginate-Chitosan-Pluronic Composite Nanoparticles for Delivery to Cancer Cells. *Na-*

nomedicine: *Nanotechnology*, *Biology*, *and Medicine*, **6**, 153-160. https://doi.org/10.1016/j.nano.2009.05.009

[6] Nooshkam, M. and Varidi, M. (2020) Maillard Conjugate-Based Delivery Systems for the Encapsulation, Protection, and Controlled Release of Nutraceuticals and Food Bioactive Ingredients: A Review. *Food Hydrocolloids*, **100**, Article No. 105389. https://doi.org/10.1016/j.foodhyd.2019.105389

[7] Banerjee, A., Qi, J., Gogoi, R., Wong, J. and Mitragotri, S. (2016) Role of Nanoparticle Size, Shape and Surface Chemistry in Oral Drug Delivery. *Journal of Controlled Release*, **238**, 176-185. https://doi.org/10.1016/j.jconrel.2016.07.051

[8] Kim, E.S., Lee, J-S. and Lee, H.G. (2016) Nanoencapsulation of Red Ginseng Extracts Using Chitosan with Polyglutamic Acid or Fucoidan for Improving Antithrombotic Activities. *Journal of Agricultural and Food Chemistry*, **64**, 4765-4771. https://doi.org/10.1021/acs.jafc.6b00911

[9] Teng, Z., Luo, Y., Li, Y. and Wang, Q. (2016) Cationic Beta-Lactoglobulin Nanoparticles as a Bioavailability Enhancer: Effect of Surface Properties and Size on the Transport and Delivery *in Vitro*. *Food Chemistry*, **204**, 391-399. https://doi.org/10.1016/j.foodchem.2016.02.139

[10] Chang, Y. and McClements, D.J. (2014) Optimization of Orange Oil Nanoemulsion Formation by Isothermal Low-Energy Methods: Influence of the Oil Phase, Surfactant, and Temperature. *Journal of Agricultural and Food Chemistry*, **62**, 2306-2312. https://doi.org/10.1021/jf500160y

[11] Hosseini, S.F., Zandi, M., Rezaei, M. and Farahmandghavi, F. (2013) Two-Step Method for Encapsulation of Oregano Essential Oil in Chitosan Nanoparticles: Preparation, Characterization and *in Vitro* Release Study. *Carbohydrate Polymers*, **95**, 50-56. https://doi.org/10.1016/j.carbpol.2013.02.031

[12] Keawchaoon, L. and Yoksan, R. (2011) Preparation Characterization and *in Vitro* Release Study of Carvacrol-Loaded Chitosan Nanoparticles. *Colloids and Surfaces B*: *Biointerfaces*, **84**, 163-171. https://doi.org/10.1016/j.colsurfb.2010.12.031

[13] Qin, Y., Wen, Q., Cao, J., Yin, C., Chen, D. and Cheng, Z. (2015) Flavonol Glycosides and Other Phenolic Compounds from *Viola tianshanica* and Their Anti-Complement Activities. *Pharmaceutical Biology*, **54**, 1140-1147. https://doi.org/10.3109/13880209.2015.1055635

[14] Nobossé, P., Fombang, E.N. and Mbofung, C.MF. (2017) The Effect of Steam Blanching and Drying Method on Nutrients, Phytochemicals and Antioxidant Activity of Moringa (*Moringa oleifera* L.) Leaves. *American Journal of Food Science and Technology*, **5**, 53-60.

[15] Brand-Williams, W., Cuvelier, S.E. and Berset, C. (1995) Use of a Free Radical Method to Evaluate Antioxidant Activity. *Lebensm-Wiss Technol*, **28**, 25-30. https://doi.org/10.1016/S0023-6438(95)80008-5

[16] Re, R., Pellegrini, N., Proteggente, A., Ananth, P., Yang, M. and Rice-Evans, C. (1999) Antioxidant Activity Applying an Improved ABTS Radical Cation Decolorization Assay. *Free Radical Biology & Medicine*, **26**, 1231-1237. https://doi.org/10.1016/S0891-5849(98)00315-3

[17] Prieto, P., Pineda, M. and Aguilar, M. (1999) Spectrophotometric Quantitation of Antioxidant Capacity through the Formation of Phosphomolybdenum Complex: Specific Application to Determination of Vitamin E. *Analytical Biochemistry*, **269**, 337-341. https://doi.org/10.1006/abio.1999.4019

[18] Yen, G.C. and Chen, H.Y. (1995) Antioxidant Activity of Various Teas Extracts in Relation to Their Antimutagenicity. *Journal of Agricultural and Food Chemistry*,

43, 27-32. https://doi.org/10.1021/jf00049a007

[19] Davidov-Pardo, G., Gumus, C.E. and McClements, D.J. (2016) Lutein-Enriched Emulsion-Based Delivery Systems: Influence of pH and Temperature on Physical and Chemical Stability. *Food Chemistry*, **196**, 821-827. https://doi.org/10.1016/j.foodchem.2015.10.018

[20] Lertsutthiwong, P., Noomun, K., Jongaroonngamsang, N., Rojsitthisak, P. and Nimmannit, U. (2008) Preparation of Alginate Nanocapsules Containing Turmeric Oil. *Carbohydrate Polymers*, **74**, 209-214. https://doi.org/10.1016/j.carbpol.2008.02.009

[21] Arifin, D.Y., Lee, L.Y. and Wang, C-H. (2006) Mathematical Modeling and Simulation of Drug Release from Microspheres: Implications to Drug Delivery Systems. *Advanced Drug Delivery Reviews*, **58**, 1274-1325. https://doi.org/10.1016/j.addr.2006.09.007

[22] Costa, P. and Lobo, J.M.S. (2001) Modeling and Comparison of Dissolution Profiles. *European Journal of Pharmaceutical Sciences*, **113**, 123-133. https://doi.org/10.1016/S0928-0987(01)00095-1

[23] Marcela, V.-J., Mused, A.M. and Luz, F.M. (2017) Bioactive Components in *Moringa oleifera* Leaves Protect against Chronic Disease. *Antioxidants*, **6**, Article No. 91. https://doi.org/10.3390/antiox6040091

[24] Vázquez León, L.A., Páramo Calderón, D.E., Robles Olvera, V.J., Valdés Rodríguez, O.A., Pérez Vázquez, A., García Alvarado, M.A. and Rodríguez Jimenes, G.C. (2017) Variation in Bioactive Compounds and Antiradical Activity of *Moringa oleifera* Leaves: Influence of Climatic Factors, Tree Age and Soil Parameters. *European Food Research & Technology*, **243**, 1593-1608. https://doi.org/10.1007/s00217-017-2868-4

[25] Verma, A.R., Vijayakumar, M., Chandra, S.M. and Chandana, V.R. (2009) *In Vitro* and *in Vivo* Antioxidant Properties of Different Fractions of *Moringa oleifera* Leaves. *Food and Chemical Toxicology*, **47**, 2196-2201. https://doi.org/10.1016/j.fct.2009.06.005

[26] Zhang, D., Xie, L., Jia, G., Cai, S., Ji, B., Liu, Y., Wu, W., Zhou, F., Wang, A., Chu, L., Wei, Y., Liu, J. and Gao, F. (2011) Comparative Study on Antioxidant Capacity of Flavonoids and Their Inhibitory Effects on Oleic Acid-Induced Hepatic Steatosis *in Vitro*. *European Journal of Medicinal Chemistry*, **46**, 4548-4558. https://doi.org/10.1016/j.ejmech.2011.07.031

[27] Bhattacharjee, S. (2016) DLS and Zeta Potential—What They Are and What They Are Not? *Journal of Controlled Release*, **235**, 337-351. https://doi.org/10.1016/j.jconrel.2016.06.017

[28] He, C., Yin, L., Tang, C. and Yin, C. (2012) Size-Dependent Absorption Mechanism of Polymeric Nanoparticles for Oral Delivery of Protein Drugs. *Biomaterials*, **33**, 8569-8578. https://doi.org/10.1016/j.biomaterials.2012.07.063

[29] Shah, P., Parameswara, R.V., Sanjay, K.S., Achint, J. and Sanjay, S. (2014) Pharmacokinetic and Tissue Distribution Study of Solid Lipid Nanoparticles of Zidovudine in Rats. *Journal of Nanotechnology*, **2014**, Article ID: 854018. https://doi.org/10.1155/2014/854018

[30] Mora-Huertas, C.E., Fessi, H. and Elaissari, A. (2010) Polymer-Based Nanocapsules for Drug Delivery. *International Journal of Pharmaceutics*, **385**, 113-142. https://doi.org/10.1016/j.ijpharm.2009.10.018

[31] McClements, D.J. (2011) Edible Nanoemulsions: Fabrication, Properties, and Functional Performance. *Soft Matter*, **7**, 2297-2316.

https://doi.org/10.1039/C0SM00549E

[32] Joye, I.J. and McClements, D.J. (2014) Biopolymer-Based Nanoparticles and Microparticles: Fabrication, Characterization, and Application. *Current Opinion in Colloid & Interface Science*, **19**, 417-427. https://doi.org/10.1016/j.cocis.2014.07.002

[33] Lee, S.S., Lee, Y.B. and Oh, I.J. (2015) Cellular Uptake of Poly (DL-lactide-co-glycolide) Nanoparticles: Effects of Drugs and Surface Characteristics of Nanoparticles. *Journal of Pharmaceutical Investigation*, **45**, 659-667. https://doi.org/10.1007/s40005-015-0221-0

[34] Gazori, T., Khoshayand, M.R., Azizi, E., Yazdizade, P., Nomani, A. and Haririan, I. (2009) Evaluation of Alginate/Chitosan Nanoparticles as Antisense Delivery Vector: Formulation, Optimization and *in Vitro* Characterization. *Carbohydrate Polymers*, **77**, 599-606. https://doi.org/10.1016/j.carbpol.2009.02.019

[35] Tan, C., Xue, J., Abbas, S., Feng, B., Zhang, X. and Xia, S. (2014) Liposome as a Delivery System for Carotenoids: Comparative Antioxidant Activity of Carotenoids as Measured by Ferric Reducing Antioxidant Power, DPPH Assay and Lipid Peroxidation. *Journal of Agricultural and Food Chemistry*, **62**, 6726-6735. https://doi.org/10.1021/jf405622f

[36] Surh, J., Decker, E.A. and McClements, D.J. (2017) Utilisation of Spontaneous Emulsification to Fabricate Lutein Loaded Nanoemulsion-Based Delivery Systems: Factors Influencing Particle Size and Colour. *International Journal of Food Science and Technology*, **52**, 1408-1416. https://doi.org/10.1111/ijfs.13395

[37] Silva, H.D., Cerqueira, M.Â. and Vicente, A.A. (2012) Nanoemulsions for Food Applications: Development and Characterization. *Food Bioprocess Technology*, **5**, 854-867. https://doi.org/10.1007/s11947-011-0683-7

[38] Paul, W. and Sharma, C.P. (2012) Synthesis and Characterization of Alginate Coated Zinc Calcium Phosphate Nanoparticles for Intestinal Delivery of Insulin. *Process Biochemistry*, **47**, 882-886. https://doi.org/10.1016/j.procbio.2012.01.018

[39] Cruz, L., Soares, L.U., Costa, T.D., Mezzalira, G., da Silveira, N.P., Guterres, S.S. and Pohlmann, A.R. (2006) Diffusion and Mathematical Modeling of Release Profiles from Nanocarriers. *International Journal of Pharmaceutics*, **313**, 198-205. https://doi.org/10.1016/j.ijpharm.2006.01.035

[40] Cauchetier, E., Deniau, M., Fessi, H., Astier, A. and Paul, M. (2003) Atovaquone-Loaded Nanocapsules: Influence of the Nature of the Polymer on their *in Vitro* Characteristics. *International Journal of Pharmaceutics*, **250**, 273-281. https://doi.org/10.1016/S0378-5173(02)00556-2

[41] Yang, R., Sun, G., Zhang, M., Zhou, Z., Li, Q., Strappe, P. and Blanchard, C. (2016) *Epigallocatechin gallate* (EGCG) Decorating Soybean Seed Ferritin as a Rutin Nanocarrier with Prolonged Release Property in the Gastrointestinal Tract. *Plant Foods for Human Nutrition*, **71**, 277-285. https://doi.org/10.1007/s11130-016-0557-2

[42] Limayem, I., Charcosset, C., Sfar, S. and Fessi, H. (2006) Preparation and Characterization of Spironolactone-Loaded Nanocapsules for Paediatric Use. *International Journal of Pharmaceutics*, **325**, 124-131. https://doi.org/10.1016/j.ijpharm.2006.06.022

[43] Siepmann, J. and Siepmann, F. (2020) Sink Conditions Do Not Guarantee the Absence of Saturation Effects. *International Journal of Pharmaceutics*, **577**, Article ID: 119009. https://doi.org/10.1016/j.ijpharm.2019.119009